Journal of Solid State Electrochemistry (2021) 25:1453–1460
https://doi.org/10.1007/s10008-021-04925-x

ORIGINAL PAPER

Effect of anodic oxygen evolution on cell morphology of sulfuric acid anodic alumina films

Katsiaryna Chernyakova[1] · Igor Vrublevsky[2] · Arunas Jagminas[1] · Vaclovas Klimas[1]

Received: 5 October 2020 / Revised: 14 February 2021 / Accepted: 18 February 2021 / Published online: 28 February 2021

Abstract

The purpose of this work was to study and analyze the effect of electrolyte temperature and anodization voltage on cell morphology of thin films of sulfuric acid anodic alumina formed on substrates of different nature, such as SiO_2/Si, glass-ceramic, glass substrates, and polished aluminum. The data obtained demonstrated that the thermal conductivity of the substrate in the voltage range from 12 to 14 V affected a pore diameter (d_{pore}) in anodic films. Depending on the substrate type, d_{pore} increased in the following order: glass > glass-ceramic > SiO_2/Si > aluminum. It was found that the anodizing voltage (U_a) of 16 V was a turning point for anodic films obtained in sulfuric acid after which the slope of the lines for both d_{pore} and D_{inter} (interpore distance) vs. U_a changed. This behavior might be explained by the occurrence of the overpotential enough for the beginning of the oxygen evolution reaction. We assumed that the oxygen evolution on aluminum oxide surface at the pore bottom at $U_a > 16$ V results in an increase in acid concentration in the solution and, consequently, in rise in acidic nature of the electrolyte and increase in the dissolution rate of the oxide layer of pore walls.

Keywords Porous oxide films · Anodic alumina · Sulfuric acid · Cell morphology · Mechanical stresses · Pore diameter · Oxygen evolution

Introduction

A model for coupled electrical migration as well as the stress-driven transport or plastic flow models is used to explain the formation of the porous structure anodic alumina [1–7]. According to this model, the volume expansion of aluminum oxide during anodic oxidation of aluminum causes the mechanical stresses in the oxide layer. As is known, the atomic density of aluminum in alumina is 2 times lower than the one in aluminum before anodizing. Hence, during the formation of anodic oxide, there exists a volume expansion of anodic film relative to the initial thickness of the film. Volume expansion increases from 1.1 to 1.6 for porous anodic alumina film with increasing anodizing voltage (U_a) [8–13]. It was shown that with increasing U_a, the volume expansion of anodic oxide can approach its theoretical limit of 2, which corresponded to the formation of aluminum oxide without any mechanical stresses. Therefore, anodizing voltage increases as well as volume expansion, while mechanical stress disappears. Skeldon et al. [3, 14], using experimental data on the change in the distribution profile of tungsten in the marker layer created in the initial aluminum film, showed that the development and growth of porous anodic alumina film occurred as a result of the movement of a viscous oxide flow from the bottom pores toward the pore walls due to plastic deformations in the oxide layer. In the case of anodizing of aluminum with a smaller number of copper impurities [15–17], the formation of ordered gas-filled voids in the pore walls of anodic aluminum oxide (horizontal pores) took place. It was found that mechanical stress determined the distance between horizontal pores in the same way as it did in the case of vertical pores [15]. Such a relationship between horizontal and vertical pores was explained by stress induced by plastic flow in anodic alumina.

It is well known that the structure of the porous anodic alumina film is determined by both a pore diameter (d_{pore}) and an interpore distance (D_{inter}). In [18], for porous anodic alumina films formed in various acids, it was shown that the

✉ Igor Vrublevsky
vrublevsky@bsuir.edu.by

[1] Center for Physical Sciences and Technology, Saulėtekio Av. 3, LT-10257 Vilnius, Lithuania

[2] Belarusian State University of Informatics and Radioelectronics, P. Brovka Str. 6, 220013 Minsk, Belarus

slope of the line in a graph of D_{inter} versus U_a was independent of acid nature. This indicates that in addition to anodizing voltage and type of electrolyte, the process of formation of the structure of porous anodic alumina films can be also influenced by non-electrochemical parameters such as mechanical stresses.

It has been found that for anodic oxide films formed in oxalic acid, the linear dependence of D_{inter} on U_a has two sections: (1) at $U_a < 30$ V with a small slope of the line and (2) at $U_a > 30$ V with a larger slope of the line [19–22]. In [22], the authors suggested that, at $U_a > 30$ V, the dissipation of the Joule heating generated in the barrier layer switched completely to the electrolyte circulating in the pore channels. At the same time, the authors did not explain this behavior for the plot of D_{inter} versus U_a. In our view, the oxygen evolution reaction (OER) during aluminum anodizing might also affect the process of formation of cell morphology [23–27].

The present work aimed to study the peculiarities of the formation of cell morphology of anodic alumina films in sulfuric acid in a wide range of anodizing voltages and determine the voltage above which the oxygen generation starts. The findings obtained for the formation of cell morphology of porous anodic alumina are explained by the effect of mechanical stress appearing in the oxide layer and the start of oxygen evolution on the oxide surface at the pore bottom during aluminum anodizing.

Experimental

Thin aluminum films of about 100 nm thick were obtained by deposition of aluminum on the silicon substrate with a thin silicon dioxide film (SiO_2/Si wafers), on glass-ceramic and glass substrates through thermal evaporation in a vacuum, and on polished aluminum substrates (0.6 mm thick). All substrates were of different thermal conductivity: 149, 1.4, 1.0, and 200 W m^{-1} K^{-1} for silicon, glass-ceramic, glass, and aluminum, respectively.

The aluminum samples were prepared by mechanical polishing, etching, then pickling using electropolishing in EtOH-glycerol-$HClO_4$ solution at 5–10 °C at 20 V for 3 min, followed by etching in 0.4-M $NaHCO_3$ at 80 °C for 60 s and rinsing in water. Then, samples were immersed in a 1.8-M aqueous solution of sulfuric acid and anodized in a potentiostatic mode in the voltage range of 12–20 V using a PI50-1 power supply. Anodizing area of 3.14 cm^2 was set by Viton o-ring. The process was carried out in a two-electrode fluoroplastic cell, similar to the one described in [22], at a constant temperature in the range of 5–40 °C. The electrolyte temperature was maintained using a WK 230 cryostat (Lauda). A platinum grid was used as a cathode. The electrolyte during anodizing was intensively stirred. The appearance of different samples after aluminum anodizing is shown in Fig. 1.

The surface morphology of porous anodic alumina films was studied by scanning electron microscopy (SEM) using a Model Quatra 200F electron microscope (FEI), followed by statistical image analysis using ImageJ software. From the results of the analysis, the values of d_{pore} and D_{inter} were determined as described in [22]. Values of d_{pore} and D_{inter} were used to graph the distribution histograms, which were further approximated by Gaussian curves. The maximum in the curves corresponded to d_{pore} and D_{inter} (Fig. 2). For the accuracy of results, we analyzed each image at least 10 times. Each time, a new pore was chosen as the reference one. The error in determining d_{pore} and D_{inter} did not exceed 2.0%.

SEM images of anodic alumina films on SiO_2/Si substrates obtained at a constant voltage of 16 V were used to study the effect of electrolyte temperature on the surface morphology. For these samples, the pore diameter was larger than that for the films obtained at lower voltages, which improved image processing in ImageJ and raised the accuracy of results. Besides, the time of complete oxidation of aluminum films did not exceed 50 s in all experiments, which prevented etching of pores at the oxide/electrolyte interface.

Results and discussion

Effect of anodizing conditions on cell morphology

According to the SEM data, in the electrolyte temperature range of 5–40 °C, the values of d_{pore} and D_{inter} equaled to (9.0 ± 0.1) nm and (43.0 ± 0.5) nm, respectively, and turned out to be independent of the electrolyte temperatures (Fig. 3). This result agrees with the data reported in [22, 28], where the effect of electrolyte temperature on the structure of porous anodic alumina films in oxalic acid was studied.

Analysis of SEM images of anodic alumina films formed on SiO_2/Si, glass-ceramic, and glass substrates and aluminum in sulfuric acid at 18 °C was used to study the effect of thermal conductivity of substrates on the surface morphology. An increase in the anodizing voltage from 12 to 14 V leads to an increase in d_{pore} from 7.5 to 8.5 nm (SiO_2/Si substrate), from 7.6 to 8.2 nm (aluminum), from 8.0 to 8.5 nm (glass-ceramic), and from 8.3 to 9.0 nm (glass) (Fig. 4). For anodic films formed at 16 and 20 V, d_{pore} was independent of the type of substrate and was 9.0 and 12.0 nm, respectively. It should be also noted that d_{pore} at $U_a < 16$ V is greater for anodic films formed on the glass substrate than that for the films formed on glass-ceramic, SiO_2/Si substrates, and aluminum (Fig. 4).

Therefore, it can be assumed that at lower anodizing voltages, d_{pore} depends on the type of substrate, in particular on its thermal conductivity. That behavior indicates that at $U_a < 16$ V, Joule heating dissipation occurs in the substrate. At $U_a > 16$

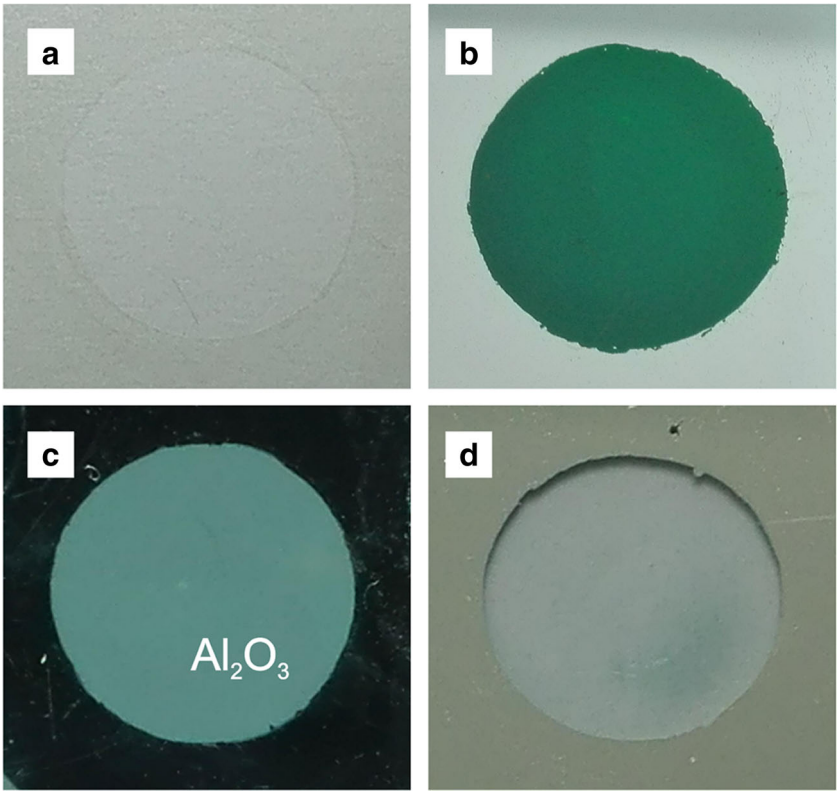

Fig. 1 Surface appearance of the as-anodized alumina films formed on aluminum substrate (**a**), SiO_2/Si substrate (**b**), glass-ceramic substrate (**c**), and **d** glass by anodizing thin aluminum films in a 1.8-M aqueous solution of sulfuric acid at 16 V and 18 °C

V, d_{pore} depends only on the anodizing voltage, and in this case, the thermal conductivity of the substrate does not affect the cell morphology of anodic alumina films (see Fig. 4). Therefore, in this case, Joule heating dissipation occurs in the electrolyte circling in the channels of pores. Thus, during anodizing of thin aluminum films in a solution of sulfuric acid, the voltage of 16 V is a turning point after which the formation process of cell morphology of anodic alumina films changes. This conclusion can be also confirmed by the graphs of D_{inter} and J_a versus U_a (Figs. 4 and 5). As can be seen from Fig. 5,

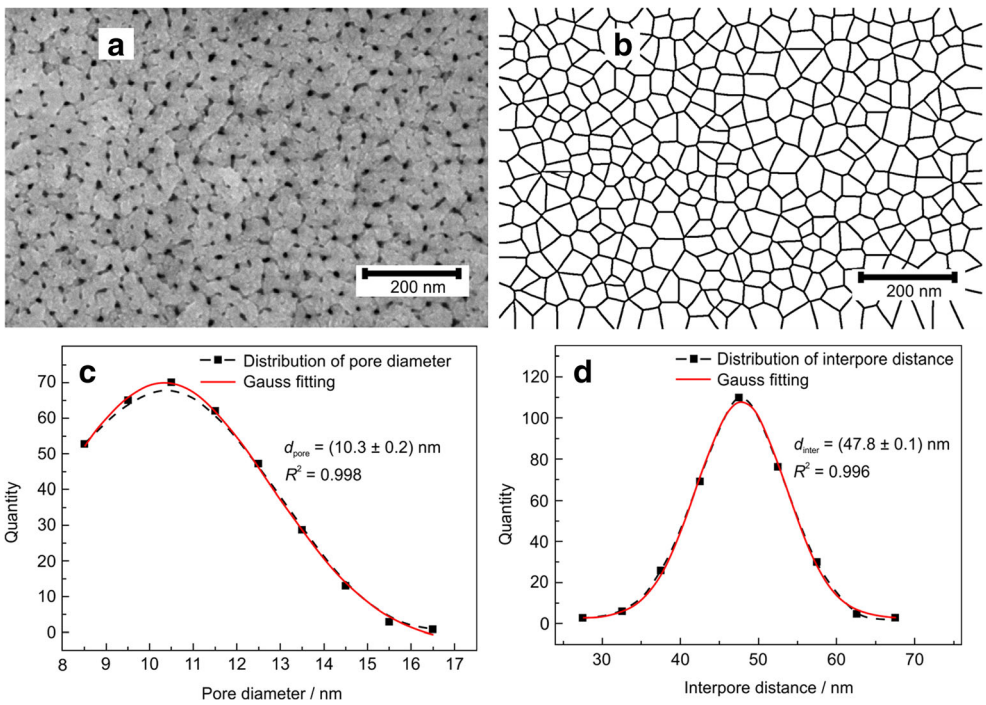

Fig. 2 Representation of the image processing steps: the original image (**a**), the segmented image showing the cells (**b**), Gaussian distribution of the pore diameter (**c**), and Gaussian distribution of interpore distance (**d**). Porous anodic alumina film was formed on SiO_2-Si substrate by the anodizing thin aluminum film in a 1.8-M aqueous solution of sulfuric acid at 18 V and 18 °C

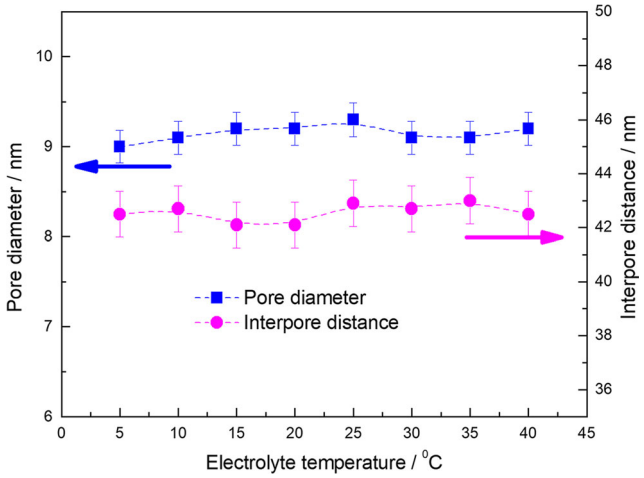

Fig. 3 Evolution of pore diameter and interpore distance as a function of the electrolyte temperature for porous alumina films formed in a 1.8-M sulfuric acid at 16 V. Porous anodic alumina films were formed by anodizing the aluminum deposited onto SiO_2/Si substrate

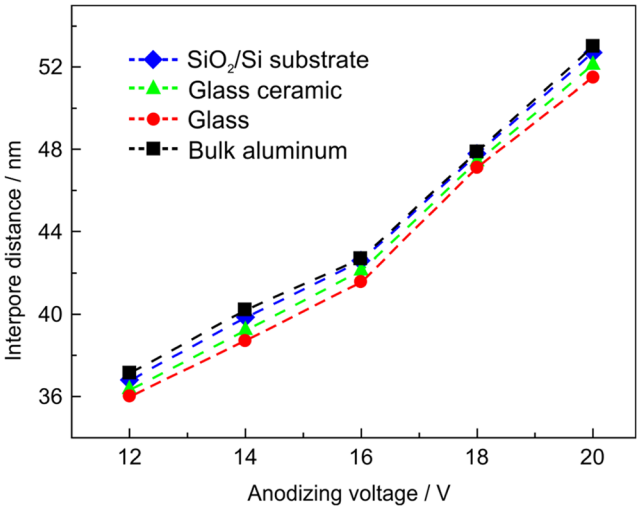

Fig. 5 Evolution of interpore distance as a function of anodizing voltage for porous anodic alumina films formed on an aluminum substrate, Si/SiO_2 substrate, glass-ceramic substrate, and glass by the anodizing thin aluminum film in a 1.8-M sulfuric acid

D_{inter} linearly increased with increasing U_a and did not depend on the type of substrate on which anodic alumina film was formed. Moreover, the slope of the line in a graph of D_{inter} versus U_a ($k = 1.45$) at the 10–16 V was less than that at 16–20 V ($k = 2.52$). The same behavior of D_{inter} was found earlier in [22]. The linear graph of D_{inter} versus U_a in the range of 10–16 V (SiO_2/Si substrate) is described by Eq. (1):

$$D_{inter} = 1.45U_a + 19.5 \quad (1)$$

and, at $U_a > 16$ V, by Eq. (2):

$$D_{inter} = 2.52U_a + 2.3 \quad (2)$$

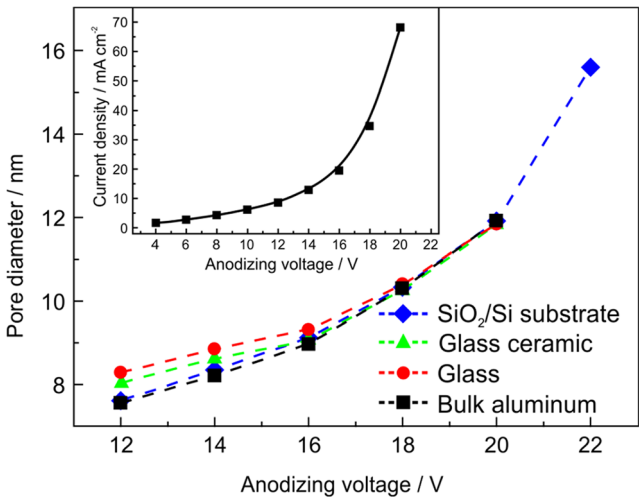

Fig. 4 Evolution of pore diameter as a function of the anodizing voltage for porous anodic alumina films formed on an aluminum substrate, SiO_2/Si substrate, glass-ceramic substrate, and glass in a 1.8-M sulfuric acid. The inset shows the evolution of current density as a function of anodizing voltage

In the U_a range of 12–16 V, J_a gradually increases with the anodizing voltage; however, at $U_a > 16$ V, the increase in J_a with the anodizing voltage is an exponential function (Fig. 4).

Effect of thermal conductivity of substrate on D_{inter}

The experimental results for porous anodic alumina films formed in sulfuric acid show that D_{inter} depends on the substrate material and, in particular, on its thermal conductivity (see Fig. 5). With a decrease in the thermal conductivity of the substrate, D_{inter} decreases in the following order ($U_a = 14$ V): 40.2 nm for the aluminum substrate (λ = 200 W m^{-1} K^{-1}), 40.0 nm for the SiO_2/Si substrate (λ = 149 W m^{-1} K^{-1}), 39.2 nm for the glass-ceramic substrate (λ = 1.4 W m^{-1} K^{-1}), and 38.7 nm for the glass substrate (λ = 1.0 W m^{-1} K^{-1}). The data obtained agree with [22].

The results can be explained based on the model of plastic deformation of the oxide layer during anodizing of aluminum. According to the model, pore walls of anodic alumina are formed by the viscosity of the barrier layer toward the cell walls and, therefore, D_{inter} results from a plastic flow of oxide under a strong electric field [3, 5, 29, 30]. As it is known, during aluminum anodizing, Joule heating is released, which is accompanied by local heating of the barrier layer at the pore bottom to the temperature, which is dependent on the rate of heat transfer [22, 31–35]. In a multilayer structure such as porous oxide layer/aluminum film/substrate, the main element that affects the rate of heat dissipation is the substrate itself because of its greater thickness. Therefore, the higher the thermal conductivity of the substrate is, the lower is the local increase in the surface temperature of the barrier oxide layer, compared with the temperature of the substrate. As it is also known, in the Al_2O_3/Al structure, the substrate is much

thicker than the aluminum layer and the layer of anodic alumina. As a result, the temperature coefficient of linear expansion (TEC) of such a structure will be determined by the TEC of the substrate only. Local heating of the barrier layer and increase in its temperature relative to the substrate, followed by restriction for expansion, cause compressive thermal stresses in the Al_2O_3 layer [7, 36]. Compressive stresses slow down the plastic deformation of anodic oxide. Therefore, with an increase in the thermal conductivity of the substrate and thereby a decrease in the local increase in the temperature of the barrier layer, the compressive stresses decrease. As a result, the plastic deformation of the oxide layer and respectively D_{inter} in the porous anodic alumina film increases. This conclusion is completely consistent with the results for D_{inter} on the thermal conductivity of the substrate. A higher D_{inter} was obtained for anodic alumina films grown on aluminum, and vice versa, a lower D_{inter} was detected for anodic films grown on a glass substrate.

Effect of anodic oxygen evolution on cell morphology of porous anodic alumina films

Anodic alumina growth during aluminum anodizing takes place due to the joint migration of Al^{3+} and O^{2-} ions in the electric field through the aluminum oxide layer. Al^{3+} cations are delivered to the electrolyte/oxide interface, forming an anodic oxide on the surface by reaction with water. In turn, O^{2-} anions are delivered at the oxide/aluminum interface, forming anodic oxide by reaction with aluminum.

In general, the electrochemical reaction $Al \rightarrow Al_2O_3$ can be written as

$$2Al + 3O^{2-} \rightarrow Al_2O_3 + 6\bar{e} \quad (3)$$

The standard electrode potential for the reaction (3) is less than for the reaction of anodic oxidation of water molecules with oxygen evolution (4)

$$H_2O \rightarrow 1/2O_2 + 2H^+ + 2\bar{e} \quad (4)$$

The standard electrode potential for OER in acidic medium is +1.23 V [37, 38]. It is worth noting that reaction (4) is endothermic. At lower U_a, only the reaction (3) takes place. It is known that the surface potential of the anodic film increases with increasing anodizing voltage [39, 40]. When the anode potential reaches the values exceeding the equilibrium potential of the oxygen electrode, water oxidation with oxygen evolution reaction starts according to the reaction (4). This data agrees with the results obtained in [24], where a significant increase in oxygen concentration on the surface of anodic alumina was observed.

As it can be seen from Fig. 5, there is a more rapid increase in the interpore distance at $U_a \geq 16$ V for anodic films on all types of substrates compared to $U_a < 16$ V. We suggest that the reason behind is the onset of oxygen evolution. After the beginning of the generation of oxygen, the heat from the anodic oxide surface is transferred to electrolyte due to the endothermic character of the reaction of anodic oxidation of water molecules with the release of oxygen. As a result, the conditions for heat dissipation from the heated surface of anodic alumina are improved and its temperature decreases. As it has been shown above, the result of this process is an increase in D_{inter} for anodic films.

It is worth noting that at U_a above 16 V, the substrate material no longer affects the pore diameter of the anodic film (see Fig. 4). This effect results from the complete dissipation of Joule heating into the electrolyte circulating in the pore channels due to the endothermic character of OER. When the OER starts on the surface of anodic oxide, the concentration of the acid increases at the pore bottom of the oxide cell and causes an increase in the acidic character of the electrolyte and increase in the dissolution rate from the pore walls.

Change in the proportionality constant of D_{inter}/U_a with anodizing voltage

In [41], the development of D_{inter} corresponding to the different stages of hard aluminum anodizing in the sulfuric acid based on SEM results of surface morphology of porous anodic alumina films was studied. In this work, the proportionality constant of D_{inter}/U_a was plotted as a function of the anodizing voltage and analyzed. It was assumed that the proportionality constant tended to a steady-state in the self-ordering growth modes of porous anodic alumina film and was equal to 1.8 nm V^{-1} in the voltage range of 40–80 V. It can be expected that an analysis of the behavior of the proportionality constant in our case can also provide valuable information on the self-organized growth modes.

As it can be seen from Fig. 6, D_{inter}/U_a decreases from 3.6 to 3.1 nm V^{-1} with increasing voltage and reaching a point at 16 V, after which a plateau for all types of substrates is observed. Depending on the substrate type, the proportionality constant in the plateau section is in the range of 2.65–2.57 nm V^{-1}.

It can be assumed that by increasing the anodizing voltage, the mechanical stresses which cause a plastic deformation of the barrier oxide layer decrease. This can be a result of the increasing pore diameter (film porosity), which corresponds to a decrease in D_{inter}/U_a with a simultaneous increase in U_a. As shown above, starting from 16 V, the conditions for oxygen evolution arise at the surface of the barrier oxide layer. From this point with further increase in U_a, the sharp drop in D_{inter}/U_a ends and D_{inter}/U_a goes to the plateau. It is worth noting that the highest value of D_{inter}/U_a (about 2.67 nm V^{-1} at 16 V) was observed for the films formed on the aluminum substrate. This may indicate the higher level of mechanical stresses in the barrier oxide layer of porous anodic alumina on aluminum

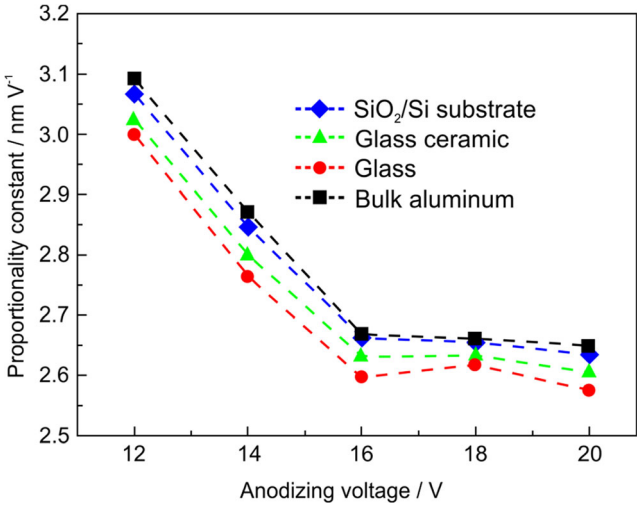

Fig. 6 Change in the proportionality constant of D_{inter}/U_a with anodizing voltage for porous anodic alumina films formed on an aluminum substrate, SiO_2/Si substrate, glass-ceramic substrate, and glass by the anodizing thin aluminum film in a 1.8-M sulfuric acid

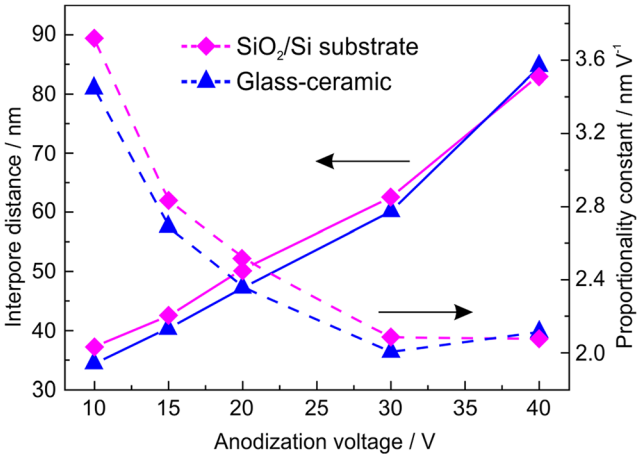

Fig. 7 Evolution of interpore distance and the proportionality constant of D_{inter}/U_a as a function of anodizing voltage for porous anodic alumina films formed on SiO_2/Si substrate and glass-ceramic substrate by the anodizing thin aluminum film in a 0.3-M oxalic acid

substrate, in comparison with other types of substrates. In turn, the minimum value of D_{inter}/U_a (about 2.60 nm V^{-1} at 16 V) was detected for anodic films formed on glass substrates. This result indicates that in this case, there was a lower level of mechanical stresses in the barrier oxide layer comparing to the samples on other types of substrates.

As it was shown above, after reaching 16 V, the barrier oxide layer of porous anodic alumina has a steady-state surface temperature, independent of the increase in anodizing voltage due to Joule heating dissipation in the electrolyte circling in the channels of pores. With increasing voltage, the rate of oxygen gas evolution increases and electrolyte aggressiveness increases as its concentration increases. As a result, compressive thermal stresses in the barrier layer will remain constant and do not limit the plastic deformation of the oxide layer with increasing voltage. Therefore, after 16 V, D_{inter} increases rapidly with increasing voltage. These suggestions are completely consistent with our results (see Fig. 6), which show that above 16 V D_{inter}/U_a for anodic oxide films on all types of substrates was independent of the anodizing voltage. It can be assumed that D_{inter}/U_a values of 2.57–2.65 nm V^{-1} for the plateau characterize the level of residual mechanical stresses in the barrier layer of porous anodic alumina films formed in sulfuric acid on various types of substrates. The smaller the value of D_{inter}/U_a in the plateau for D_{inter}/U_a versus U_a plot is, the smaller are the residual mechanical stresses in the barrier layer.

For comparison, Fig. 7 shows the plot of D_{inter}/U_a versus U_a, for anodic oxide films formed in oxalic acid. The graph has the same special characteristics as the graph for anodic alumina films formed in sulfuric acid (see Fig. 6). One can see the first section with a sharp decrease in D_{inter}/U_a with increasing voltage followed by the second section with a plateau above 30 V (30 V is a point of onset of oxygen evolution). A lower value of D_{inter}/U_a (2.0–2.1 nm V^{-1}) in the plateau indicates a lower level of residual mechanical stresses in the barrier layer in the case of oxalic acid comparing to anodic alumina films formed in sulfuric acid (2.6–2.65 nm V^{-1}). We assume that this result can be explained by the peculiarity of the structure of porous anodic alumina film formed in oxalic acid, namely the pore diameter of the film formed in oxalic acid is larger than for the one formed in sulfuric acid.

Conclusions

It was established that during anodizing of thin aluminum films at low voltages in sulfuric acid (up to 14 V), the pore diameter depended on the substrate type, especially on its thermal conductivity. With an increasing thermal conductivity of the substrate, the d_{pore} of anodic films increased in the following order: glass > glass-ceramic > SiO_2/Si > aluminum. At $U_a \geq 16$ V, only d_{pore} depended on the anodizing voltage and thermal conductivity of the substrate, and anodizing voltage did not affect the cell morphology of the films. The results obtained indicate that for porous anodic alumina films formed at $U_a < 16$ V in sulfuric acid, the dissipation of Joule heating generated during anodizing of aluminum occurs mainly by a substrate.. When anodic films are formed at $U_a \geq 16$ V, the Joule heating is dissipated by the electrolyte circulating in the pore channels.

A model of plastic deformation of oxide layer during anodizing of aluminum was used to explain the effect of thermal conductivity of the substrate on D_{inter}. It was demonstrated that with higher thermal conductivity of the substrate, the local increase in the temperature of the barrier oxide layer decreases which, in its turn, leads to a decrease in compressive thermal stresses in anodic films. It indicates that plastic deformation of

the barrier oxide layer of a growing anodic oxide film increases, followed by an increase in D_{inter} for porous anodic films. The data obtained demonstrate that U_a of 16 V was a turning point after which the formation process of the cell morphology of anodic alumina changed.

It was shown that when the anode potential reaches values exceeding the equilibrium potential of the oxygen electrode, the process of oxidation of water molecules began with the release of oxygen from the solution on the surface of the aluminum oxide at the pore bottom.

When the oxygen evolution reaction on the surface of anodic oxide through oxidation of water molecules takes place, the concentration of the acid at the pore bottom increases and causes an increase in the level of acidic character of the electrolyte and increase in the dissolution rate from the pore walls.

References

1. Jessensky O, Müller F, Gösele U (1998) Self-organized formation of hexagonal pore arrays in anodic alumina. Appl Phys Lett 72(10): 1173–1175
2. Houser JE, Hebert KR (2009) The role of viscous flow of oxide in the growth of self-ordered porous anodic alumina films. Nat Mater 8(5):415–420
3. Garcia-Vergara SJ, Skeldon P, Thompson GE, Habazaki H (2006) A flow model of porous anodic film growth in aluminium. Electrochim Acta 52(2):681–687
4. Garcia-Vergara SJ, Skeldon P, Thompson GE, Habazaki H (2007) Stress generated porosity in anodic alumina formed in sulphuric acid electrolyte. Corros Sci 49(10):3772–3782
5. Hebert KR, Houser JE (2009) A model for coupled electrical migration and stress-driven transport in anodic oxide films. J Electrochem Soc 156(8):C275–C281
6. Knörnschild G, Poznyak AA, Karoza AG, Mozalev (2015) A effect of the anodization conditions on the growth and volume expansion of porous alumina films in malonic acid electrolyte. Surf Coat Tech 275:17–25
7. Liao J, Ling Z, Li Y, Hu X (2016) The role of stress in the self-organized growth of porous anodic alumina. ACS Appl Mater Inter 8(12):8017–8023
8. Zhou F, Mohamed Al-Zenati AK, Baron-Wiecheć A, Curioni M, Garcia-Vergara SJ, Habazaki H, Skeldon P, Thompson GE (2011) Volume expansion factor and growth efficiency of anodic alumina formed in sulphuric acid. J Electrochem Soc 158(6):C202–C214
9. Vrublevsky I, Parkoun V, Sokol V, Schreckenbach J, Marx G (2004) The study of the volume expansion of aluminum during porous oxide formation at galvanostatic regime. Appl Surf Sci 222(1-4):215–225
10. Vrublevsky I, Parkoun V, Schreckenbach J, Marx G (2003) Effect of the current density on the volume expansion of he deposited thin films of aluminum during porous oxide formation. Appl Surf Sci 220(1-4):51–59
11. Vrublevsky I, Parkoun V, Schreckenbach J, Marx G (2004) Study of porous oxide film growth on aluminum in oxalic acid using a re-anodizing technique. Appl Surf Sci 227(1-4):282–292
12. Li AP, Müller F, Birner A, Nielsch K, Gösele U (1998) Hexagonal pore arrays with a 50–420 nm interpore distance formed by self-organization in anodic alumina. J Appl Phys 84(11):6023–6026
13. Arurault L (2008) Pilling–Bedworth ratio of thick anodic aluminium porous films prepared at high voltages in H_2SO_4 based electrolyte. Trans Inst Met Finish 86(1):51–54
14. Skeldon P, Thompson GE, Garcia-Vergara S, Iglesias-Rubianes L, Blanco-Pinzon CE (2006) A tracer study of porous anodic alumina. Electrochem Solid-State Let 9(11):B47–B51
15. Vanpaemel J, Abd-Elnaiem A, Gendt SDE, Vereecken PM (2015) The formation mechanism of 3D porous anodized aluminum oxide templates from an aluminum film with copper impurities. J Phys Chem C 119(4):2105–2112
16. Molchan IS, Molchan TV, Gaponenko NV, Skeldon P, Thompson GE (2010) Impurity-driven defect generation in porous anodic alumina. Electrochem Commun 12(5):693–696
17. Skeldon P, Thompson GE, Wood GC, Zhou X, Habazaki H, Shimizu K (1997) Evidence of oxygen bubbles formed within anodic films on aluminium-copper alloys. Philos Mag A 76(4):729–741
18. Lee W, Park SJ (2014) Porous anodic aluminum oxide: anodization and templated synthesis of functional nanostructures. Chem Rev 114(15):7487–7556
19. Ono S, Masuko N (2003) Evaluation of pore diameter of anodic porous films formed on aluminum. Surf Coat Tech 169-170:139–142
20. Stępniowski WJ, Norek M, Michalska-Domańska M, Bojar Z (2013) Ultra-small nanopores obtained by self-organized anodization of aluminum in oxalic acid at low voltages. Mater Lett 111:20–23
21. Sulka GD, Stępniowski WJ (2009) Structural features of self-organized nanopore arrays formed by anodization of aluminum in oxalic acid at relatively high temperatures. Electrochim Acta 54(14):3683–3691
22. Chernyakova K, Vrublevsky I, Klimas V, Jagminas A (2018) Effect of Joule heating on formation of porous structure of thin oxalic acid anodic alumina films. J Electrochem Soc 165(7):E289–E293
23. Li D, Zhao L, Jiang C, Lu JG (2010) Formation of anodic aluminum oxide with serrated nanochannels. Nano Lett 10(8):2766–2771
24. Torrescano-Alvarez JM, Curioni M, Skeldon P (2017) Gravimetric measurement of oxygen evolution during anodizing of aluminum alloys. J Electrochem Soc 164(13):C728–C734
25. Yang ZB, Hu JC, Li KQ, Zhang SY, Fan QH, Liu SA (2017) Advances of the research evolution on aluminum electrochemical anodic oxidation technology. IOP Conf Ser: Mater Sci Eng 283: 012003
26. Torrescano-Alvarez JM, Curioni M, Skeldon P (2018) Effects of oxygen evolution on the voltage and film morphology during galvanostatic anodizing of AA 2024-T3 aluminium alloy in sulphuric acid at −2 and 24 °C. Electrochim Acta 275:172–181
27. Torrescano-Alvarez JM, Curioni M, Zhou X, Skeldon P (2018) Effect of anodizing conditions on the cell morphology of anodic films on AA2024-T3 alloy. Surf Interface Anal 51(9):1–9
28. Sunseri C, Spadaro C, Piazza S, Volpe M, Quarto FDI (2006) Porosity of anodic alumina membranes from electrochemical measurements. J Solid State Electrochem 10(6):416–421
29. Garcia-Vergara SJ, Clere DL, Hashimoto T, Habazaki H, Skeldon P, Thompson GE (2009) Optimized observation of tungsten tracers for investigation of formation of porous anodic alumina. Electrochim Acta 54(26):6403–6411
30. Garcia-Vergara SJ, Skeldon P, Thompson GE, Habazaki H (2007) Tracer studies of anodic films formed on aluminium in malonic and oxalic acids. Appl Surf Sci 254(5):1534–1542
31. Chowdhury P, Thomas AN, Sharma M, Barshilia HC (2014) An approach for in situ measurement of anode temperature during the growth of self-ordered nanoporous anodic alumina thin films: influence of Joule heating on pore microstructure. Electrochim Acta 115:657–664

32. Aerts T, Graeve ID, Terryn H (2009) Control of the electrode temperature for electrochemical studies: a new approach illustrated on porous anodizing of aluminium. Electrochem Commun 11(12): 2292–2295
33. Aerts T, Jorcin JB, Graeve ID, Terryn H (2010) Comparison between the influence of applied electrode and electrolyte temperatures on porous anodizing of aluminium. Electrochim Acta 55(12): 3957–3965
34. Graeve ID, Terryn H, Thompson GE (2002) Influence of heat transfer on anodic oxidation of aluminium. J Appl Electrochem 32(1): 73–83
35. Schneider M, Lammel C, Heuber C, Michaelis A (2011) In situ temperature measurement on the metal/oxide/electrolyte interface during the anodizing of aluminium. Mater Corros 64:60–68
36. Çapraz ÖÖ, Shrotriya P, Skeldon P, Thompson GE, Hebert KR (2015) Factors controlling stress generation during the initial growth of porous anodic aluminum oxide. Electrochim Acta 159: 16–22
37. Kondo M, Masaoka S (2016) Water oxidation catalysts constructed by biorelevant first-row metal complexes. Chem Lett 45(11):1220–1231
38. Deng Y, Handoko AD, Du Y, Xi S, Yeo BS (2016) In situ Raman spectroscopy of copper and copper oxide surfaces during electrochemical oxygen evolution reaction: identification of Cu III oxides as catalytically active species. ACS Catal 6(4):2473–2481
39. Vrublevsky I, Chernyakova K, Bund A, Ispas A, Schmidt U (2012) Effect of anodizing voltage on the sorption of water molecules on porous alumina. Appl Surf Sci 258(14):5394–5398
40. Lambert J, Guthmann C, Ortega C, Saint-Jean M (2002) Permanent polarization and charge injection in thin anodic alumina layers studied by electrostatic force microscopy. J Appl Phys 91(11):9161–9169
41. Schwirn K, Lee W, Hillebrand R, Steinhart M, Nielsch K, Gösele U (2008) Self-ordered anodic aluminum oxide formed by H_2SO_4 hard anodization. ACS Nano 2(2):302–310